Free Vibration Analysis of Rhombic Plate with Central Crack

Mohammad Sikandar Azam, Vinayak Ranjan and Bipin Kumar

Department of Mechanical Engineering, Indian Institute of Technology (Indian School of Mines), Dhanbad–826004, India.

(Received 29 January 2015; accepted 5 May 2016)

In this paper, free vibration analysis of rhombic plate with pre-existing central crack has been done using the finite element method. The Mindlin theory of plate has been used in the process of investigation. The following six boundary conditions at the edges of the plate have been considered. They are simply supported at all edges (SSSS), clamped at all edges (CCCC), free at all edges (FFFF), clamped-simply supported (CSSC), clamped-free (CFFC), and clamped-free-simply supported (CSFS). Effects of crack length on natural frequencies of rhombic plate with different skew angles i.e. 15°, 30°, 45°, 60° have been studied. It is observed that percentage drop in fundamental frequency due to presence of central crack in the rhombic plate increases with an increase in skew angle for CCCC, SSSS, and CSSC edge conditions at a given crack ratio (non-dimensional crack length). Under the CFFC, CSFS, and FFFF edge conditions, percentage drop in natural frequency of rhombic plate is very small for crack ratio of 0.2 at different skew angles. In case of the CFFC edge condition of the rhombic plate, percentage drop in fundamental frequency is within 0.7% at all skew angles and with all crack ratios considered. Some of the results obtained by the present method have been compared with the published results. Most of the results obtained are novel for rhombic crack plate.

1. INTRODUCTION

Applications of skew plates are found in various types of engineering structures such as aircraft wings, bridge decks, ship decks, and rail and road vehicles. Manufacturing processes and loading conditions may induce a crack in a plated structure, which significantly alters the dynamic behaviour of the plate. Therefore, dynamic analysis of skew plate is crucial for design engineers. A substantial amount of literature is available on free vibration of intact skew plates. Leissa[1] presented a monograph on vibration of plate followed by review articles[2–4] on previous work carried out in the field of plate vibration. Different methods have been applied to solve the problem of free vibration of skew plates under simply supported edge condition. Raju and Hinton[5] examined natural frequencies and mode shape of the rhombic Mindlin plate under various boundary conditions containing simply supported and clamped edges using quadrilateral isoparametric plate element. They explained the effect of skew angles and thickness ratio on mode frequency of the plate. Durvasula[6,7] applied the Ritz method and the Galerkin method to determine natural frequencies under simply supported and clamped edge conditions. Liew and Lam[8] adopted Rayleigh-Ritz method along with two-dimensional orthogonal plate function to work out natural frequencies of the skew plate under varied edge conditions and at different skew angles. Liew et al.[9] delved into the phenomenon of vibration of skew plates based on Mindlin plate theory under simply supported edge condition and for two opposite edges simply supported with the other two clamped. Stress singularities at the obtuse corner were first used by Basu et al.[10] They modelled the quadrant at 60° simply supported skew plate using hierarchical Legendre elements of the fifth order. Mc Gee[11,12] tried to get to the bottom of vibration of cantilever skew plate considering the plate to be thick and with singularity at the corner. Huang et al.[13] investigated the plate vibration considering stress singularities at the obtuse corner of a simply supported skew plate using Ritz method. They applied displacement function consisting of algebraic polynomial and the corner function that takes care of corner stress singularity. Mc Gee et al.[14] studied the effect of stress singularity at the corner on the vibration of skew (rhombic) plate with different combinations of simply supported and clamped edges conditions. Langrangian function was obtained by the Ritz method. Transverse displacement function was constructed by making use of the algebraic polynomial and corner function, which account for kinematic boundary condition and stress singularity at the hinged -hinged and clamped-hinged corners. Further Mc Gee et al.[15] investigated the singularity effect on vibration behaviour of skew plate under free and simply supported edge conditions. Woo et al.[16] determined natural frequencies and mode shapes of a skew Mindlin plate using P-version of the finite element method under different sets of boundary conditions and discussed the effect of skew angle, aspect ratio, and cutout dimension on the frequency parameter. Zhou and Zheng[17] came out with accurate results on vibration of skew plate by utilizing moving least square - Ritz method. Results, thus obtained, were found close to the available results in literature but certain mode frequencies deviated from the data presented by Mc Gee et al.,[12] Hung et al.,[13] and Mc Gee et al.[15] Mizusawa and Kondo[18] investigated vibration of the skew plate with linearly varied thickness along longitudinal axis by using the spline spring method. By making use of the differential quadrature method as well as polynomial and harmonic functions, Malekzadeh and Karami[19] analysed free vibration of skew plate with linearly varying thickness in both directions. Based on linear and small strain theory of elasticity in three dimensions, Zhou et al.[20] studied the vibration of thick skew plate. Eigenvalue equation was obtained from energy functional using the Ritz method. Displacement function was formed by multiplying Chebyshev polynomial series with boundary function. Lai et al.[21] adopted DSC-element method to analyse vibration of skew plates by using the first order shear deformation theory for continuous and discontinuous boundaries. Wang and Wu[22] studied the free vibration of skew under 14 sets of boundary condition with free edges by applying modified differential quadrature method (DQM). The authors observed that problems were extremely sensitive to grid spacing and to the method of applying the multiple boundary condition at large skew angle. Wang et al.[23] further investigated the skew plate vibration phenomenon by utilizing a new version of DQM under eight sets of edge conditions consisting of free, simply supported, and clamped.

The studies referred above focus to vibration characteristic of intact skew plate. Vibration of cracked rectangular and square plates was studies by various researchers but the literature on vibration of cracked skew plate is merely available. Stahl and Keer,[24] Huang and Leissa,[25] Huang et al.,[26] Bachene et al.,[27] and Liew et al.[31] studied the vibration of cracked rectangular and square plate with central crack, side crack and inclined crack under different boundary conditions by different methods that include the Ritz method, Rayleigh-Ritz method and finite element method. Recently, Israr et al.,[28] Ismail and Cartmell,[29] and Joshi et al.[30] presented closed form solution for the vibration of cracked rectangular plate. This paper deals with the effect of central crack on natural frequencies of skew plate under six different combinations of edge conditions by the finite element method.

2. METHODOLOGY

2.1. Formulation of Rectangular Plate with Crack

Let us consider an isotropic square plate with central crack in Cartesian coordinate system as shown in Fig. 1. The crack is continuous line through crack. Formulations of the displacement and the finite element equation are based upon the Mindlin plate‘s theory, which take into account shear deformation and rotary inertia. Let u, v, w are the displacement in x, y, and z direction respectively, then

$$u(x, y, z) = z\theta_x(x, y); \tag{1}$$

$$v(x, y, z) = z\theta_y(x, y); \tag{2}$$

$$w(x, y, z) = w_z(x, y); \tag{3}$$

where θ_x and θ_y are the rotations of the mid surface normal in x-z and y-z planes respectively.

We assume that crack path is parallel to one side of the plate and the crack stops at the end of each element as depicted in Fig. 1. The discretization of the plate may be represented by[27,32]

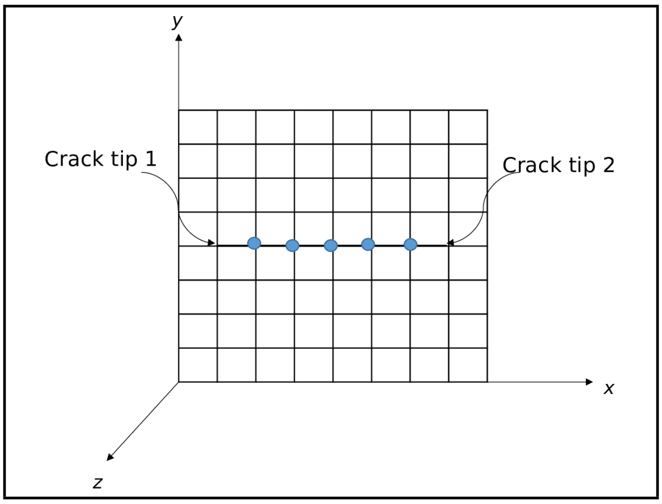

Figure 1. Discretization of plate (crack aligned with mesh, circle nodes are enriched with jump function).

$$\{\delta\} = \sum_i [N_i]\{\delta_i\} + \sum_j H(x)[N_j]\{\delta'_j\}. \tag{4}$$

In Eq. (4), N_i and δ_i are the classical shape function and the classical nodal displacements, respectively, at node i. Next, j represents the nodes at discontinuity, and δ'_j are the nodal displacements to be enriched and $H(x)$ is a discontinuity function. Based upon Mindlin plate theory, finite element formulation can be written as

$$\{\delta\} = \begin{Bmatrix} w_z \\ \theta_x \\ \theta_y \end{Bmatrix} = \sum_I [N_i]\{\delta_i\} + \sum_J H[N_j]\{\delta'_j\}. \tag{5}$$

I is set of all nodal points on the plate, J is set of all nodes of elements located on the discontinuity and

$$\{\delta_i\} = \begin{Bmatrix} w_{zi} \\ \theta_{xi} \\ \theta_{yi} \end{Bmatrix}; \tag{6a}$$

$$\{\delta'_j\} = \begin{Bmatrix} w'_{zj} \\ \theta'_{xj} \\ \theta'_{yj} \end{Bmatrix}. \tag{6b}$$

The strain field ε_{xx}, ε_{yy}, γ_{xy}, γ_{xz}, and γ_{yz} can be written in matrix form as in Eq. (7) (See on top of the next page). The Eq. (7) can be symbolically written as follows

$$\{\varepsilon\} = [B_i]\{\delta_i\} + [B'_j]\{\delta'_j\}; \tag{8}$$

where $[B'_j] = H[B_j]$.

The stress field can be written as

$$\{\sigma\} = [D][B_i]\{\delta_i\} + [D][B'_j]\{\delta'_j\}; \tag{9}$$

where $[D]$ represents elastic coefficient matrix and $\{\sigma\}$ is generalized stress.

The potential energy of any element e of the plate is given by

$$U^e = \frac{1}{2}\int_{A_e} \{\sigma\}^T\{\varepsilon\} dA; \tag{10}$$

$$\varepsilon_{ij} = \begin{Bmatrix} \varepsilon_{xx} \\ \varepsilon_{yy} \\ \gamma_{xy} \\ \gamma_{xz} \\ \gamma_{yz} \end{Bmatrix} = \sum_I \begin{bmatrix} 0 & \frac{\partial [N_i]}{\partial x} & 0 \\ 0 & 0 & \frac{\partial [N_i]}{\partial y} \\ 0 & \frac{\partial [N_i]}{\partial y} & \frac{\partial [N_i]}{\partial x} \\ \frac{\partial [N_i]}{\partial x} & [N_i] & 0 \\ \frac{\partial [N_i]}{\partial x} & 0 & [N_i] \end{bmatrix} \begin{Bmatrix} w_{zi} \\ \theta_{xi} \\ \theta_{yi} \end{Bmatrix} + \sum_J \begin{bmatrix} 0 & H\frac{\partial [N_j]}{\partial x} & 0 \\ 0 & 0 & H\frac{\partial [N_j]}{\partial y} \\ 0 & H\frac{\partial [N_j]}{\partial y} & H\frac{\partial [N_j]}{\partial x} \\ H\frac{\partial [N_j]}{\partial x} & H[N_j] & 0 \\ H\frac{\partial [N_j]}{\partial x} & 0 & H[N_j] \end{bmatrix} \begin{Bmatrix} w'_{zj} \\ \theta'_{xj} \\ \theta'_{yj} \end{Bmatrix}. \tag{7}$$

$$U^e = \frac{1}{2} \int_{A_e} \left(\{\delta_i\}^T [B_i]^T [D] + \{\delta'_j\}^T [B'_j]^T [D] \right) \left([B_i]\{\delta_i\} + [B'_j]\{\delta'_j\} \right) dA; \tag{11}$$

where A_e = element area.

Equation (11) can be further written as

$$U^e = \frac{1}{2} \left\{ \{\delta_i\}^T \{\delta'_j\}^T \right\} [K^e] \begin{Bmatrix} \delta_i \\ \delta'_j \end{Bmatrix}; \tag{12}$$

where

$$[K^e] = \begin{bmatrix} \int_A [B_i]^T [D][B_i] dA & \int_A [B_i]^T [D][B'_j] dA \\ \int_A [B'_j]^T [D][B_i] dA & \int_A [B'_j]^T [D][B'_j] dA \end{bmatrix}; \tag{13a}$$

or

$$[K^e] = \begin{bmatrix} [K^e_{ii}] & [K^e_{ij}] \\ [K^e_{ji}] & [K^e_{jj}] \end{bmatrix}; \tag{13b}$$

where $[K^e_{ii}]$ is classical stiffness matrix, $[K^e_{ij}]$, and $[K^e_{ji}]$ are coupling stiffness matrix, and $[K^e_{jj}]$ is enriched stiffness matrix.

The kinetic energy for an element of the plate is given by

$$[T^e] = \frac{1}{2} \int \{\dot{\delta}_e\}^T \rho \{\dot{\delta}_e\} h dA; \tag{14}$$

where $\dot{\delta}_e$ is the first derivative of the displacement field w.r.t time and ρ is the material density of the plate.

Similarly, by proper transformation Eq. (14) may also be written as

$$T^e = \frac{1}{2} \left\{ \{\dot{\delta}_i\}^T \{\dot{\delta}'_j\}^T \right\} [M^e] \begin{Bmatrix} \dot{\delta}_i \\ \dot{\delta}'_j \end{Bmatrix}; \tag{15}$$

where $[M^e]$ of the element is given as

$$[M^e] = \begin{bmatrix} \int_{A_e} [N_i] \rho [N_i] h dA & \int_{A_e} [N_i] \rho H [N_j] h dA \\ \int_{A_e} H[N_j] \rho [N_i] h dA & \int_{A_e} H[N_j] \rho H [N_j] h dA \end{bmatrix}; \tag{16a}$$

or

$$[M^e] = \begin{bmatrix} [M^e_{ii}] & [M^e_{ij}] \\ [M^e_{ji}] & [M^e_{jj}] \end{bmatrix}. \tag{16b}$$

Here, $[M^e_{ii}]$ is the classical mass matrix, $[M^e_{ij}]$ and $[M^e_{ji}]$ are the coupling mass matrix, and $[M^e_{jj}]$ is enriched mass matrix.

2.2. Oblique Boundary Transformation

Figure 2 shows the geometry and co-ordinate system of rhombic plate where a and b are equal. Next, c indicates the crack length, and β is the skew angle of the skew plate.

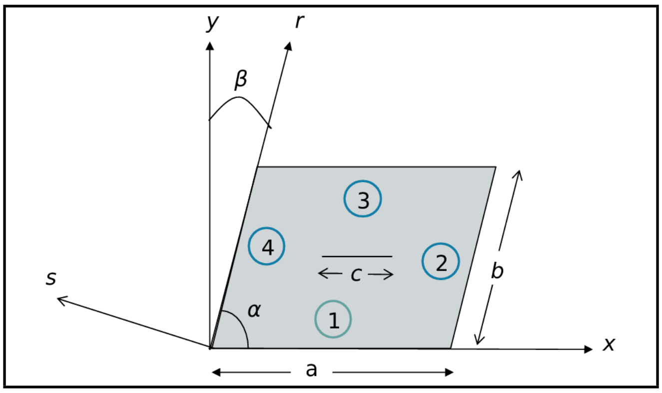

Figure 2. Geometry and co-ordinate system of rhombic plate.

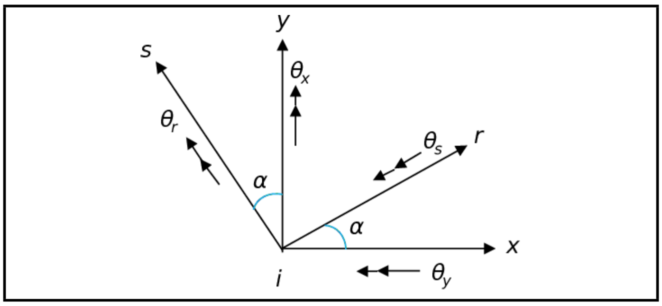

Figure 3. Global and local skew co-ordinate system for oblique boundary transformation.

For skew plate, both the edges may not be parallel to the global axes x and y. To specify the boundary conditions at such edges the local displacements w, θ_r, and θ_s as shown in Fig. 3 may be used.

Here, θ_r and θ_s are average rotations of the normal to the reference plane and are tangential and normal to the oblique edge. It is necessary to transform the element matrices corresponding to global axes (x, y) along which the boundary conditions are specified.

Using θ_x, θ_y, θ_r, and θ_s vector as shown in Fig. 3, where $\alpha = 90° - \beta$, the displacement transformation for a node i on the oblique boundary is given by

$$\{\delta\} = \begin{Bmatrix} w_z \\ \theta_x \\ \theta_y \end{Bmatrix} = \begin{bmatrix} 1 & 0 & 0 \\ 0 & \cos\alpha & -\sin\alpha \\ 0 & \sin\alpha & \cos\alpha \end{bmatrix} \begin{Bmatrix} w_z \\ \theta_r \\ \theta_s \end{Bmatrix} = [R] \begin{Bmatrix} w_z \\ \theta_r \\ \theta_s \end{Bmatrix}; \tag{17}$$

where $[R]$ is transformation matrix. This matrix is valid for three degrees of freedom per node. For nodes which are not located on the oblique boundary, it becomes a unit matrix.

The element stiffness matrix and the mass matrix are then arrived at after mapping into the (r, s) co-ordinate system as

$$[\mathcal{K}^e] = \int_{A_e} [R]^T [K^e][R] dA; \tag{18}$$

$$[\mathcal{M}^e] = \int_{A_e} [R]^T [M^e][R] dA. \tag{19}$$

The free vibration equation of the skew plate with crack can be written as

$$[\mathcal{K}] - \{\lambda\}[\mathcal{M}]\{\delta\}_{r,s} = 0; \tag{20}$$

where $\{\lambda\}$, $[\mathcal{K}]$, and $[\mathcal{M}]$ are eigenvalues, assembled stiffness matrix, and assembled mass matrix, respectively.

3. NUMERICAL RESULTS AND DISCUSSION

The approach discussed in preceding section has been applied to study free vibration of a rhombic plate with central crack as shown in Fig. 2 under different combinations of edge conditions. Skew plate having all the edges equal in length $(a = b)$ is called a rhombic plate. Natural frequencies are presented in terms of non-dimensional frequency parameters formulated as

$$\Omega = \omega a^2 \sqrt{\frac{\rho h}{\mathcal{D}}}; \tag{21}$$

where $\mathcal{D}$ is the bending rigidity given by $Eh^3/[12(1 - \nu^2)]$. Further, ρ, E, and ν are density, Young‘s modulus, and Poisson‘s ratio, respectively, of the plate material. Next, h represents the thickness of the plate.

The present problem uses density ρ, Young‘s modulus E, and Poisson‘s ratio ν of the plate material equal to 7800 kg/m^3, 200 GPa, and 0.3 respectively. Throughout, the analysis thickness to length ratio (h/a) of the plate has been kept equal to 0.001. Both intact skew plate and cracked skew plates with central crack parallel to the edge along x axis of the plate have been studied under six different combination of edge conditions as described in Table 1 with reference to Fig. 2. Crack length in terms of crack ratio has been used throughout the present investigation, which is defined as ratio of crack length c and edge length a along x axis.

3.1. Validation of Results

First, frequency parameters for intact rhombic plate are tabulated under different set of edge conditions. Table 1 displays the comparison of first five frequency parameters obtained through the present formulation with the results achieved by Wang and Wu[22] for rhombic intact plate with skew angles 15°, 30°, 45°, and 60° under the FFFF edge condition. The frequency parameters $\Omega = \omega a^2 \sqrt{\rho h/\mathcal{D}}$ are in very good agreement. The frequency parameters of FFFF rhombic plate with skew angle 30° and 60° are also compared with those obtained by Singh and Chakerverty.[34] Large deviation in frequency parameter can be observed at large skew angle. Clearly, results obtained by them[34] are not converged at high skew angle. Table 3 shows that frequency parameters of the rhombic plate with different skew angles under SSSS edge condition agree well with the ones from Wang et al.,[23] Woo et al.,[16] Liew et al.,[9] Huang et al.,[13] and Bardell.[33] For the skew angle of 60°, first mode frequency of the rhombic plate is slightly more than that obtained by Wang et al.[23] and Huang et al.[13] but slightly less than that obtained by Woo et al.,[16] Liew et al.,[9] and Bardell.[33] Differences in results are more for mode 5 but the present results are close to those given by Bardell[33] for all modes. Results of intact rhombic plate under CCCC edge conditions are compared with those obtained from the investigation of Wang et al.,[23] Woo et al.,[16] Liew et al.,[9] Raju and Hinton,[5] and Bardell.[33] The comparisons are shown in Table 4. Good agreement between the results can be seen. From the above discussion, it can be concluded that present model provides very good results for intact rhombic plate with different skew angle under different edge conditions. However, it still requires confirmation regarding crack plate.

To validate the present model for crack plate, simply supported plate with central crack is considered. Table 5 shows that the frequency parameters of a square plate with central crack under simply supported edge condition are in very close agreement with those obtained by Bechene et al.[27] and Stahl and Keer[24] and agree well with those given by Huang et al.,[26] and Liew et al.[31] Huang et al.[26] and Liew et al.[31] have adopted Ritz method and domain decomposition method, respectively, to investigate the vibration of crack plate. Their results are slightly on the higher side. Although results for six and seven modes are also available in literature for few cases but the comparisons are made up to 5$^{\text{th}}$ mode only for the sake of uniformity. Apart from the five lowest natural frequencies used for validation, results for the sixth and seventh mode frequencies are also presented in Tables 2 to 5.

This paper presents new sets of results of frequency parameters for cracked skew plates with different skew angles under SSSS, FFFF, CCCC, CFFC, CSSC, and CSFS edge conditions as described in Tables 6 to 9.

3.2. Intact Rhombic Plate

This section, first, analyses the effect of skew angle on natural frequencies of rhombic plate when the skew angle changes from 15° to 60° with an interval of 15°. Figure 4 shows the effect of skew angle on fundamental frequency of rhombic intact plate. An increase in skew angle from 0° to 60° results in an increase in fundamental frequencies of rhombic plate under SSSS, CCCC, CSSC, and CSFC edge conditions while fundamental frequency of rhombic plate decreases under FFFF edge conditions. In case of CFFC rhombic plate, fundamental frequency remains almost the same with variation of skew angle. The increase in frequency parameter with an increase in skew angle is greater when the skew angle goes beyond 45° under SSSS, CCCC, and CSSC edge conditions of the rhombic plate. Again, it can be observed from Tables 6 to 9 that higher modes frequencies (mode 2 onward) of the rhombic plate under SSSS, CCCC, CSSC, and CSFC conditions go up with an increase in skew angle. In case of CFFC edge condition, higher mode (mode 3 onward) frequencies go on increasing with an increase

Table 1. Description of six edge conditions.

Edge conditions	Edge 1	Edge 2	Edge 3	Edge 4
SSSS	Simply supported	Simply supported	Simply supported	Simply supported
FFFF	Free	Free	Free	Free
CCCC	Clamped	Clamped	Clamped	Clamped
CFFC	Clamped	Free	Free	Clamped
CSSC	Clamped	Simply supported	Simply supported	Clamped
CSFS	Clamped	Simply supported	Free	Simply supported

Table 2. Comparison of frequency parameters $\Omega = \omega a^2 \sqrt{\rho h/\mathcal{D}}$ for rhombic intact plate under FFFF edge condition.

Skew angle	Reference	Modes						
β °		1	2	3	4	5	6	7
15	Present	12.757	20.291	27.106	30.288	39.289	57.549	63.667
	[22]	12.761	20.292	27.108	30.298	39.304		
30	Present	11.528	22.645	26.652	35.359	43.915	51.673	69.387
	[22]	11.531	22.646	26.659	35.364	43.933		
	[34]	11.690	22.926	27.254	36.512	46.214		
45	Present	10.499	24.032	27.761	41.766	51.521	61.518	66.930
	[22]	10.499	24.034	27.763	41.771	51.537		
60	Present	9.779	22.265	39.296	39.854	62.674	68.575	89.716
	[22]	9.779	22.268	39.316	39.859	62.686		
	[34]	9.824	23.140	40.033	52.669	78.110		

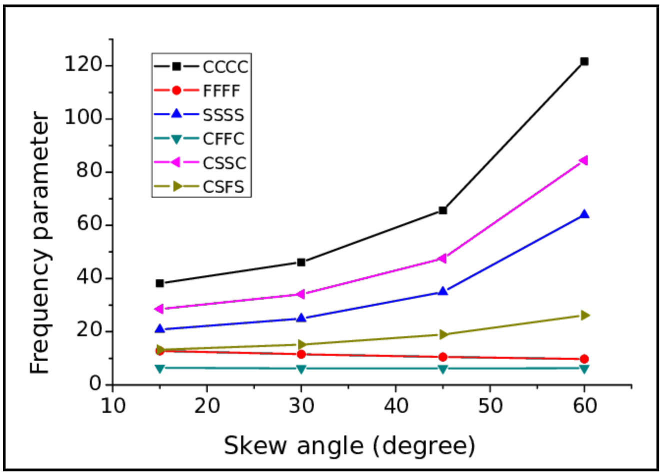

Figure 4. Effect of skew angle on fundamental frequency of intact rhombic plate.

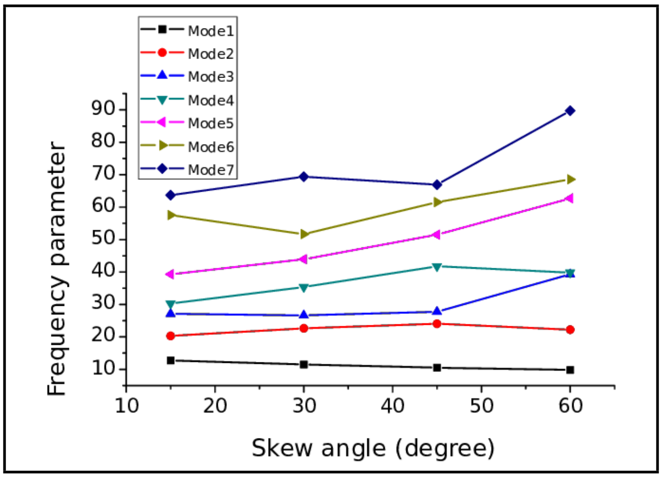

Figure 5. Effect of skew angle on natural frequencies of FFFF rhombic plate.

in skew angle. However higher modes frequencies of FFFF rhombic plate such as the 2nd, 3rd, 4th, 6th, and 7th modes, show a combination of increasing and decreasing pattern of variation in natural frequencies with an increase in skew angle as shown in Fig. 5. The 5th mode frequency of FFFF rhombic plate increases smoothly with increase in skew angle.

A change in skew angle of rhombic plate results in change in the mass of the plate as well as change in the shape of the plate. Mass of the plate directly affects its natural frequency whereas a change in the shape of the plate alters the stiffness, which ultimately changes the natural frequencies of the plate. The magnitude of the change in stiffness due to change in shape (change in skew angle) also depends upon the edge condition. Figure 4 also exhibits the effect of edge conditions on fundamental frequency of the rhombic plate. Under the CFFC edge condition, rhombic plate has the lowest fundamental frequency and under the CCCC edge conditions, it has the highest fundamental frequency among the six different combinations of edge conditions considered in this paper. This observation is true for all the skew angles of the plate considered for the analysis, such as, 15°, 30°, 45°, and 60°. The effect of edge conditions can also be studied from Tables 6 to 9. It is noticed that natural frequencies increase due to higher constraint. Frequency parameter under FFFF edge condition is lowest among SSSS, FFFF, and CCCC whereas frequency parameter of CCCC edge condition is the highest. This is due to the fact that more edge constraints result in an increase in stiffness of the plate causing an increase in natural frequencies.

3.3. Rhombic Plate with Crack

Tables 6 to 9 present the seven lowest natural frequencies for CCCC, CFFC, CSSC, FFFF, CSFS, and SSSS rhombic cracked plate with skew angles 15°, 30°, 45°, and 60°. As expected, the natural frequency decreases with an increase in crack length of rhombic plates, irrespective of the skew angles and edge conditions. The decrease in natural frequencies due to the formation of crack and further decrease in frequency due to an increase in crack ratio are attributed to reduction in local stiffness of the plate. It is further noticed that a reduction in natural frequencies of a cracked rhombic plate is not proportional to the crack ratio. A small crack with a ratio $c/a = 0.2$

Table 3. Comparison of frequency parameters $\Omega = \omega a^2 \sqrt{\rho h/\mathcal{D}}$ for rhombic intact plate under SSSS edge condition.

Skew angle	Reference	Modes						
β °		1	2	3	4	5	6	7
15	Present	20.858	48.192	56.089	79.010	103.981	108.857	120.432
	[23]	20.868	48.205	56.107	79.043	104.000		
	[16]	20.873	48.204	56.130	79.0457	104.0029		
	[9]	20.871	48.205	56.115	79.0457	103.998		
	[13]	20.868	48.205	56.107	79.0427	104.000		
30	Present	24.900	52.624	71.720	83.808	122.782	122.802	140.471
	[23]	24.899	52.638	71.711	83.829	122.820		
	[16]	25.049	52.638	72.067	83.901	122.890		
	[9]	24.964	52.638	71.871	83.858	122.820		
	[13]	24.899	52.638	71.711	83.829	122.820		
45	Present	34.935	66.266	100.287	107.446	140.766	168.275	185.066
	[23]	34.755	66.277	100.250	107.010	140.800		
	[16]	35.403	66.292	100.654	109.302	141.372		
	[9]	35.333	66.277	100.429	108.323	140.802		
	[13]	34.749	66.277	100.250	107.040	140.800		
60	Present	63.929	104.912	148.011	196.191	208.840	248.963	293.411
	[23]	62.331	104.950	147.650	196.290	205.350		
	[16]	68.258	105.230	150.230	199.990	217.820		
	[9]	66.303	104.970	148.740	196.410	213.790		
	[13]	62.409	104.950	147.670	196.290	205.860		
	[33]	64.818	104.960	148.320	196.290	210.660		

Table 4. Comparison of frequency parameters $\Omega = \omega a^2 \sqrt{\rho h/\mathcal{D}}$ for rhombic intact plate under CCCC edge condition.

Skew angle	Reference	Modes						
β °		1	2	3	4	5	6	7
15	Present	38.186	72.896	82.618	109.558	138.970	145.149	157.569
	[23]	38.187	72.896	82.618	109.560	138.970		
	[16]	38.175	72.902	82.665	109.645	139.310		
	[9]	38.186	72.895	82.616	109.558	138.970		
	[5]	38.215	73.242	83.003	110.342	141.826		
30	Present	46.092	81.602	105.166	119.251	164.983	165.315	186.178
	[23]	46.089	81.601	105.170	119.250	164.990		
	[33]	46.090	81.601	105.170	119.250	164.990		
	[9]	46.089	81.599	105.160	119.250	164.980		
45	Present	65.651	106.507	148.327	157.249	196.793	229.510	248.421
	[23]	65.643	106.490	148.310	157.230	196.770		
	[16]	65.707	106.848	150.312	159.174	203.041		
	[9]	65.652	106.491	148.316	157.264	196.795		
	[5]	65.781	107.579	151.597	158.802	204.992		
60	Present	121.634	177.710	231.729	291.496	304.732	354.605	408.631
	[23]	121.640	177.720	231.750	291.520	304.780		
	[33]	121.650	177.720	231.750	291.520	304.810		
	[9]	121.790	177.710	231.890	291.790	305.410		

reduces the first seven frequency parameters by less than 3% in relation to an intact CSSC rhombic plate with a skew angle of 15°. On the other hand, a crack ratio of 0.5 decreases the frequency parameter by up to 16% for the 5$^{\text{th}}$ mode of the CSSC skew plate. At this point of discussion percentage reduction or drop in natural frequency, Π is formulated as

$$\Pi = \frac{\Omega_{\text{uncracked}} - \Omega_{\text{cracked}}}{\Omega_{uncracked}} \times 100 \qquad (22)$$

As the skew angle of rhombic plate increases, the percentage drop in fundamental frequency increases under SSSS, CCCC, and CSSC edge conditions for a particular crack ratio as shown in Figs. 6 to 10. For small cracks ($c/a \approx$ 0.2), the percentage drop in fundamental frequency is very small in case of CFFC, CSFS and FFFF rhombic plate at all skew angles as observed in Fig. 6. When the crack ratio increases to 0.8, the percentage drop in fundamental frequency of CSFS and FFFF rhombic plate becomes obvious at higher skew angles as shown in Fig. 10. It is further noted that percentage drop in fundamental frequency for CFFC rhombic plate is negligibly small (within 0.7%) at all skew angles and all crack ratios considered in this paper. It can be observed in Figs. 6 and 7 that the line of SSSS edge condition of the rhombic plate crosses the line of the CCCC edge condition. Plates under SSSS and CCCC edge conditions, having skew angle about 47°, will have equal percentage change in fundamental frequency due to the development of crack having a crack ratio of 0.2. Similarly, plates under SSSS and CCCC edge conditions having skew angle about 32° will also have the equal percentage change in fundamental frequency due to the development of crack having crack ratio of 0.4. The trend of crossing the line of SSSS edge conditions with CCCC edge condition is not observed with the crack ratios of 0.5, 0.6, and 0.8.

Apart from the development of crack and skew angle, changes in natural frequencies also depend upon the mode

Table 5. Comparison of frequency parameters $\Omega = \omega a^2 \sqrt{\rho h/\mathcal{D}}$ for for square plate with central crack parallel to one edge of the plate.

Edge condition	Reference	Crack ratio	Modes						
			1	2	3	4	5	6	7
SSSS	[24]	0	19.739	49.348	49.348	78.957	98.696		
	[31]		19.740	49.350	49.350	78.960	98.700		
	[27]		19.739	49.348	49.348	78.955	98.698		
	Present		19.738	49.347	49.347	78.953	98.697	98.697	128.252
	[26]	0.1	19.660	49.340	49.350	78.960	97.790		
	Present		19.621	49.323	49.332	78.924	97.433	98.696	128.207
	[24]	0.2	19.305	49.170	49.328	78.957	93.959		
	[31]		19.380	49.160	49.310	78.810	94.690		
	[27]		19.305	49.181	49.324	78.945	93.893		
	[26]		19.330	49.190	49.320	78.950	94.130		
	Present		19.308	49.183	49.321	78.949	93.912	98.685	127.714
	[26]	0.3	18.850	48.500	49.240	78.890	89.730		
	Present		18.909	48.630	49.262	78.912	90.593	98.675	125.262
	[24]	0.4	18.279	46.624	49.032	78.602	85.510		
	[31]		18.440	46.440	49.040	78.390	86.710		
	[27]		18.278	46.635	49.032	78.600	85.450		
	[26]		18.290	46.650	49.030	78.610	85.560		
	Present		18.281	46.637	49.031	78.612	85.459	98.614	112.313
	[24]	0.5	17.706	43.031	48.697	77.733	82.155		
	[31]		17.850	42.820	48.720	77.440	83.010		
	[27]		17.707	43.042	48.685	77.710	82.108		
	[26]		17.720	43.060	48.690	77.720	82.180		
	Present		17.710	43.049	48.680	77.715	82.111	95.498	98.380
	[24]	0.6	17.193	37.978	48.223	75.581	79.588		
	[31]		17.330	37.750	48.260	75.230	80.320		
	[27]		17.180	37.987	48.214	75.579	79.556		
	[26]		17.190	37.990	48.220	75.590	79.600		
	Present		17.180	37.989	48.218	75.580	79.559	85.485	97.983

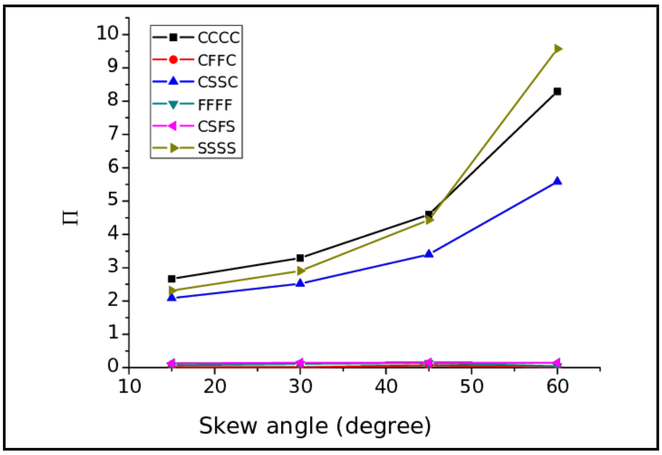

Figure 6. Effect of skew angles on percentage drop in fundamental frequency of rhombic plate for crack ratio of 0.2.

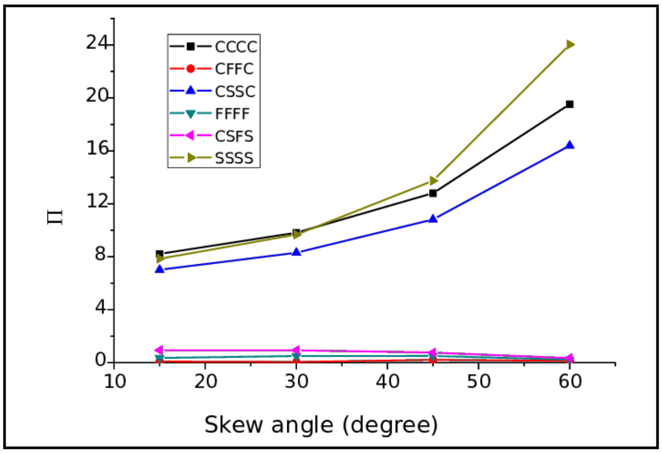

Figure 7. Effect of skew angles on percentage drop in fundamental frequency of rhombic plate for crack ratio of 0.4.

number and edge conditions of the rhombic plate. Percentage change or drop in fundamental frequency due to a change in crack ratio from zero to 0.8 is the maximum under the SSSS edge conditions and minimum under the CFFC edge condition as shown in Fig. 10. If we look at 15° rhombic plate under CCCC edge conditions, percentage drop in natural frequency is the maximum (48.59%) in second mode and minimum (12%) in third mode out of seven lowest natural frequencies for a crack ratio of 0.8.

The percentage drop in natural frequency may be used for an estimation of the magnitude of crack present in rhombic plate under different edge conditions and at different skew angles. For example, a drop in natural frequency of 19.52% in the CCCC rhombic plate with the skew angle of 60° may be estimated at a crack ratio of 0.4 (Fig. 11).

Table 6. Seven non-dimensional frequency parameters $\Omega = \omega a^2\sqrt{\rho h/\mathcal{D}}$ of a thin rhombic plate with central horizontal crack under different boundary conditions ($h/a = 0.001$, $\nu = 0.3$, $\beta = 15°$).

Edge conditions	Crack ratio	Modes 1	2	3	4	5	6	7
CCCC	0	38.186	72.896	82.618	109.558	138.970	145.149	157.569
	0.2	37.168	72.720	82.167	109.107	135.308	141.242	156.696
	0.4	35.051	68.493	77.206	107.397	124.118	137.752	140.196
	0.5	34.101	60.296	74.934	105.261	119.731	123.380	138.478
	0.6	33.395	50.828	73.725	100.787	115.938	116.988	135.214
	0.8	32.749	37.473	72.622	83.357	111.424	112.830	130.064
CFFC	0	6.443	24.780	25.248	47.499	64.269	68.382	82.163
	0.2	6.441	24.457	25.197	46.617	64.175	68.279	81.897
	0.4	6.437	23.431	25.073	44.780	62.469	67.800	78.235
	0.5	6.433	22.721	24.935	43.813	58.463	67.160	73.774
	0.6	6.429	21.932	24.705	42.509	51.841	66.418	71.240
	0.8	6.411	20.162	23.821	35.758	45.637	64.749	67.939
CSSC	0	28.557	59.919	68.320	93.546	120.854	125.943	138.384
	0.2	27.960	59.509	68.025	93.300	118.325	122.765	137.670
	0.4	26.556	57.122	64.642	91.131	107.910	120.953	127.870
	0.5	25.802	52.780	62.059	87.969	102.021	115.684	121.543
	0.6	25.121	45.965	60.632	84.066	96.957	111.674	118.161
	0.8	24.077	34.149	59.451	74.311	87.789	108.820	111.469
FFFF	0	12.757	20.291	27.106	30.288	39.289	57.549	63.667
	0.2	12.747	20.092	26.438	30.272	39.282	56.848	63.654
	0.4	12.712	19.262	24.952	29.994	39.139	55.593	62.469
	0.5	12.677	18.467	24.280	29.564	38.901	55.138	56.889
	0.6	12.622	17.402	23.787	28.745	38.403	49.311	54.797
	0.8	12.283	14.765	23.227	24.950	35.131	40.194	53.670
CSFS	0	13.264	33.432	45.129	62.104	78.850	95.129	100.545
	0.2	13.246	32.528	44.932	62.035	78.448	95.084	99.639
	0.4	13.140	30.360	44.354	60.952	72.204	94.391	98.089
	0.5	13.015	29.176	43.800	58.254	65.512	93.419	97.495
	0.6	12.821	28.088	42.648	51.833	62.100	91.287	96.884
	0.8	12.163	26.380	35.374	45.034	59.021	78.776	95.768
SSSS	0	20.858	48.192	56.089	79.010	103.981	108.857	120.432
	0.2	20.376	48.130	55.913	78.719	101.866	105.941	119.985
	0.4	19.220	46.941	53.530	77.735	93.640	105.171	111.009
	0.5	18.578	44.305	51.324	76.767	90.130	98.315	104.486
	0.6	17.983	39.330	49.844	75.074	87.141	89.614	102.833
	0.8	17.090	28.608	48.311	66.771	82.397	83.361	97.626

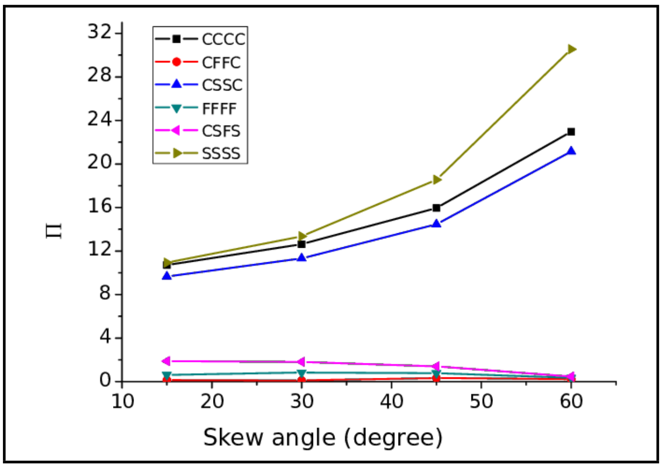

Figure 8. Effect of skew angles on percentage drop in fundamental frequency of rhombic plate for crack ratio of 0.5.

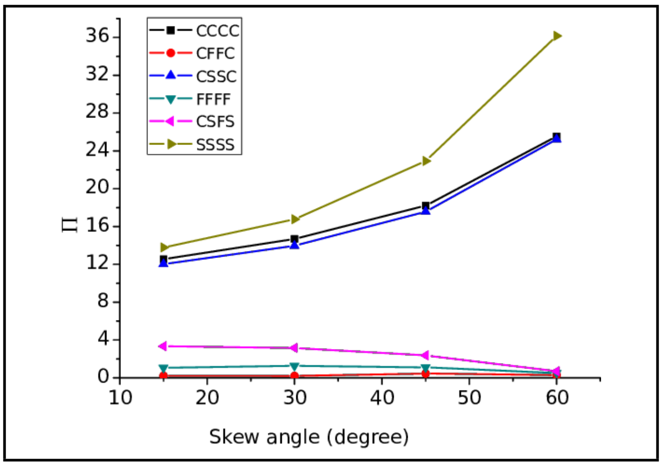

Figure 9. Effect of skew angles on percentage drop in fundamental frequency of rhombic plate for crack ratio of 0.6.

4. CONCLUSIONS

Based on Mindlin plate theory, finite element formulation was carried out to find out natural frequencies of rhombic plate with central through crack. Plates with different skew angles of 15°, 30°, 45°, and 60° under six different combinations of edge conditions i.e. CCCC, CSSC, CFFC, FFFF, CSFS, and SSSS were considered for the analysis. The finite element formulation requires enrichment of elements near crack only, and regular finite elements are used away from the crack. Numer-

Table 7. Seven non-dimensional frequency parameters $\Omega = \omega a^2 \sqrt{\rho h/\mathcal{D}}$ of a thin rhombic plate with central horizontal crack under different boundary conditions ($h/a = 0.001$, $\nu = 0.3$, $\beta = 30°$).

Edge conditions	Crack ratio	Modes						
		1	2	3	4	5	6	7
CCCC	0	46.092	81.602	105.166	119.251	164.983	165.315	186.178
	0.2	44.575	81.438	104.072	118.456	162.814	164.163	178.047
	0.4	41.561	77.436	90.569	116.799	151.587	151.763	170.567
	0.5	40.270	67.599	84.677	115.020	143.530	146.314	162.572
	0.6	39.323	56.331	82.668	110.493	139.606	142.123	150.094
	0.8	38.280	42.103	81.228	91.069	136.809	137.112	138.252
CFFC	0	6.240	24.740	28.379	49.352	71.326	75.385	88.400
	0.2	6.239	24.523	28.307	48.175	71.162	75.074	88.047
	0.4	6.237	23.804	28.053	45.855	68.525	74.274	84.542
	0.5	6.234	23.243	27.841	44.858	62.777	73.799	79.695
	0.6	6.228	22.559	27.551	43.931	54.227	73.212	76.747
	0.8	6.210	20.855	26.604	38.354	45.932	70.137	74.545
CSSC	0	34.076	66.336	86.846	100.619	143.103	143.284	161.538
	0.2	33.218	65.774	86.182	100.246	141.028	142.595	155.351
	0.4	31.244	63.560	77.382	98.188	128.785	136.042	148.659
	0.5	30.221	59.357	70.002	96.137	120.219	132.582	143.025
	0.6	29.319	51.201	66.935	93.165	115.139	128.707	134.640
	0.8	27.997	37.752	65.405	81.028	107.610	115.676	130.478
FFFF	0	11.528	22.645	26.652	35.359	43.915	51.673	69.387
	0.2	11.515	22.447	26.641	34.446	43.911	50.738	69.378
	0.4	11.470	21.662	26.449	32.089	43.792	49.246	69.153
	0.5	11.433	20.918	26.150	30.808	43.583	48.774	64.757
	0.6	11.381	19.881	25.586	29.700	43.148	48.446	53.617
	0.8	11.180	16.953	22.979	28.071	38.040	42.664	47.605
CSFS	0	15.167	35.940	55.433	64.950	94.530	98.868	119.633
	0.2	15.144	35.004	54.769	64.893	94.018	98.471	118.255
	0.4	15.024	32.704	52.669	64.060	84.246	96.974	114.864
	0.5	14.892	31.424	50.529	62.818	73.159	96.019	113.174
	0.6	14.687	30.228	46.662	60.210	65.877	93.845	112.030
	0.8	13.986	28.289	36.405	55.392	61.793	80.695	108.799
SSSS	0	24.900	52.624	71.720	83.808	122.782	122.802	140.471
	0.2	24.177	52.571	71.277	83.291	121.400	122.388	134.751
	0.4	22.492	51.558	65.151	82.200	114.064	116.184	128.945
	0.5	21.575	49.221	58.976	81.479	108.988	109.865	125.459
	0.6	20.725	43.599	55.101	80.154	103.789	106.302	118.402
	0.8	19.394	31.084	52.501	71.933	99.697	100.951	102.427

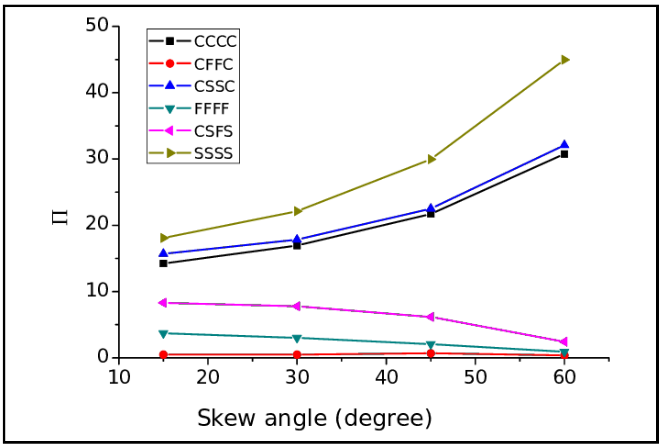

Figure 10. Effect of skew angles on percentage drop in fundamental frequency of rhombic plate for crack ratio of 0.8.

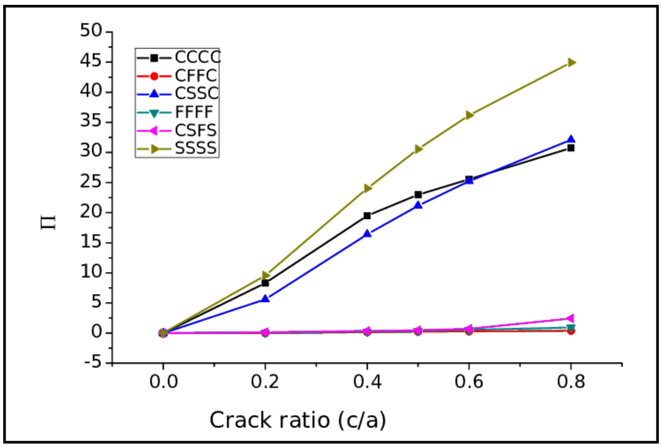

Figure 11. Effect of crack ratio on percentage drop in fundamental frequency of rhombic plate with skew angle 60°.

ical results obtained were shown extensively in the form of table to show the effect of crack and skew angle on natural frequencies of the rhombic plate. Most of the results presented forrhombic plate with central crack are first reported in literature. From the investigation of computed results of natural frequencies following may be concluded.

(i) Natural frequency decreases with an increase in the crack length irrespective of the edge conditions and skew angles of rhombic plate.

(ii) The percentage drop in fundamental frequency increases

Table 8. Seven non-dimensional frequency parameters $\Omega = \omega a^2\sqrt{\rho h/\mathcal{D}}$ of a thin rhombic plate with central horizontal crack under different boundary conditions ($h/a = 0.001$, $\nu = 0.3$, $\beta = 45°$).

Edge conditions	Crack ratio	Modes 1	2	3	4	5	6	7
CCCC	0	65.651	106.507	148.327	157.249	196.793	229.510	248.421
	0.2	62.633	106.237	147.085	153.059	195.871	226.406	248.151
	0.4	57.249	99.028	114.724	145.596	189.257	210.111	236.805
	0.5	55.179	82.266	107.290	143.419	186.538	193.521	218.255
	0.6	53.690	68.222	104.949	135.927	174.081	184.747	207.782
	0.8	51.398	53.494	102.173	109.115	165.118	175.791	199.426
CFFC	0	6.208	25.738	34.301	55.638	82.877	85.599	118.513
	0.2	6.203	25.613	34.224	54.150	81.372	85.427	117.833
	0.4	6.194	25.160	33.893	51.095	77.760	83.443	107.065
	0.5	6.187	24.764	33.578	49.848	71.625	80.843	94.309
	0.6	6.179	24.229	33.161	48.999	61.243	79.346	90.040
	0.8	6.164	22.671	31.994	45.408	49.270	76.505	86.534
CSSC	0	47.503	85.181	122.860	128.928	167.599	197.691	215.139
	0.2	45.887	84.025	122.396	126.698	166.373	194.604	214.384
	0.4	42.365	80.843	99.196	120.924	163.277	170.559	205.581
	0.5	40.640	73.811	85.870	118.972	159.669	161.235	194.883
	0.6	39.152	61.801	82.852	115.134	147.843	157.450	180.601
	0.8	36.805	46.109	80.667	96.183	133.951	149.627	164.560
FFFF	0	10.499	24.032	27.761	41.766	51.521	61.518	66.930
	0.2	10.484	24.027	27.534	4.171	51.484	57.729	66.889
	0.4	10.446	23.902	26.696	41.360	50.398	50.849	66.233
	0.5	10.418	23.703	25.894	40.761	47.507	49.684	65.065
	0.6	10.383	23.320	24.741	39.597	45.793	47.044	61.776
	0.8	10.279	21.210	21.433	36.139	37.486	44.678	54.080
CSFS	0	18.952	43.493	69.993	84.209	107.204	133.078	144.920
	0.2	18.923	42.234	68.690	83.672	106.905	131.040	144.001
	0.4	18.807	38.996	65.327	80.687	98.733	113.474	141.119
	0.5	18.688	37.070	61.916	76.476	86.231	109.697	139.794
	0.6	18.501	35.123	55.642	71.355	80.289	107.409	136.444
	0.8	17.780	31.308	43.378	67.012	74.360	93.673	115.036
SSSS	0	34.935	66.266	100.287	107.446	140.766	168.275	185.066
	0.2	33.386	66.180	99.442	105.650	140.352	166.561	184.824
	0.4	30.137	64.733	85.583	98.356	136.268	157.204	181.536
	0.5	28.456	61.038	72.007	97.814	133.685	149.036	170.170
	0.6	26.928	51.882	66.652	96.445	131.794	136.014	157.590
	0.8	24.467	35.903	62.924	84.747	113.749	128.842	146.347

for SSSS, CCCC, and CSSC rhombic plates with an increase in skew angles at agiven crack ratio.

(iii) With a small crack ratio of $c/a \approx 0.2$, the percentage drop in fundamental frequency is very small for CFFC, CSFC and FFFF rhombic plate at different skew angles.

(iv) central crack with $c/a = 0.8$ reduces the fundamental frequency only by 0.7% in relation to that of intact plate under CFFC edge condition of the rhombic plate.

(v) Fundamental frequency of rhombic intact plate remains almost the same with variation of skew angle (up to 60° has been considered in this paper) under CFFC conditions.

Although rhombic thin plate with crack were analysed herein, present methodology can be applied to treat thick plate, as the formulation is based on Mindlin plate theory, which is suitable for moderately thick plate. This approach can be applied to treat other shape of plates such as triangular plate and skew trapezoidal plate with central crack and side crack. Furthermore, it will be interesting to extend the methodology to analyse vibration of rhombic plate with multiple cracks.

REFERENCES

[1] Leissa, A. W. *Vibration of Plates*, NASA SP-160, (1969).

[2] Leissa, A. W. Recent research in plate vibrations: classical theory, *Shock and Vibration Digest*, **9** (10), 13–24, (1977). https://dx.doi.org/10.1177/058310247700901005

[3] Leissa, A. W. Plate vibrations research 1976-1980: classical theory, *Shock and Vibration Digest*, **13** (9), 11–22, (1981). https://dx.doi.org/10.1177/058310248101300905

[4] Leissa, A. W. Recent studies in plate vibrations 1981-1985: part I classical theory, *Shock and Vibration Digest*, **19** (2), 11–18, (1987). https://dx.doi.org/10.1177/058310248701900204

[5] Raju, K. K. and Hinton, E. Natural frequencies and modes of rhombic Mindlin plates, *Earthquake Engi-*

Table 9. Seven non-dimensional frequency parameters $\Omega = \omega a^2\sqrt{\rho h/\mathcal{D}}$ of a thin rhombic plate with central horizontal crack under different boundary conditions ($h/a = 0.001$, ν = 0.3, $\beta = 60°$).

Edge conditions	Crack ratio	Modes 1	2	3	4	5	6	7
CCCC	0	121.634	177.710	231.729	291.496	304.732	354.605	408.631
	0.2	111.551	176.693	228.965	274.824	290.684	352.587	402.563
	0.4	97.892	143.800	173.680	227.108	284.435	317.562	354.314
	0.5	93.689	115.401	166.869	218.476	261.612	282.844	345.846
	0.6	90.561	99.442	161.912	192.595	242.599	279.334	339.564
	0.8	84.234	84.738	150.689	153.096	234.136	240.889	320.358
CFFC	0	6.295	27.006	46.597	63.790	107.167	114.220	145.075
	0.2	6.294	26.958	46.506	62.953	102.034	114.109	141.328
	0.4	6.287	26.758	45.855	60.759	94.149	112.014	131.626
	0.5	6.281	26.555	45.223	59.628	91.024	101.283	118.103
	0.6	6.277	26.241	44.452	58.717	82.245	93.206	114.823
	0.8	6.272	25.151	42.644	57.508	63.970	89.585	106.073
CSSC	0	84.414	138.420	186.641	241.274	245.539	298.881	348.093
	0.2	79.703	134.115	185.841	231.954	238.958	297.195	332.758
	0.4	70.576	125.615	137.924	182.024	236.596	271.310	296.207
	0.5	66.570	103.329	128.387	177.009	222.585	243.607	292.353
	0.6	63.117	86.124	125.168	165.901	196.519	235.604	286.895
	0.8	65.413	67.431	115.618	132.024	186.104	207.807	253.912
FFFF	0	9.779	22.265	39.296	39.854	62.674	68.575	89.716
	0.2	9.774	22.264	39.074	39.850	62.646	68.398	89.630
	0.4	9.756	22.190	38.111	39.834	61.842	65.905	82.659
	0.5	9.744	22.067	37.118	39.813	58.668	64.064	74.426
	0.6	9.729	21.820	35.607	39.720	51.788	63.441	67.722
	0.8	9.688	20.438	30.684	37.726	38.728	57.467	62.805
CSFS	0	26.198	62.600	97.101	138.638	146.379	186.903	224.672
	0.2	26.160	60.780	92.554	137.830	144.251	185.604	216.414
	0.4	26.106	55.084	85.665	119.518	134.927	151.919	186.292
	0.5	26.075	50.935	83.221	96.445	129.277	143.653	183.574
	0.6	26.017	46.219	79.240	83.078	122.589	139.593	171.937
	0.8	25.561	37.044	64.946	78.083	110.095	127.456	134.808
SSSS	0	63.929	104.912	148.011	196.191	208.840	248.963	293.411
	0.2	57.811	104.621	145.777	194.042	196.826	247.203	290.553
	0.4	48.565	99.975	117.919	144.641	191.820	242.463	259.587
	0.5	44.403	84.542	101.054	143.882	189.790	209.546	246.597
	0.6	40.804	66.881	95.846	140.061	173.163	188.703	240.717
	0.8	35.185	45.822	86.961	110.706	148.040	180.740	220.645

neering and Structural Dynamics, **8**, 55–62, (1980). https://dx.doi.org/10.1002/eqe.4290080106

6 Durvasula, S. Free vibration of simply supported parallelogrammic plates, *Journal of Aircraft*, **6** (1), 61–68, (1969). https://dx.doi.org/10.2514/3.44005

7 Durvasula, S. Natural frequencies and modes of clamped skew plates, *American Institute of Aeronautics and Astronautics Journal*, **7** (6), 1164–1166, (1969). https://dx.doi.org/10.2514/3.5296

8 Liew, K. M. and Lam, K. Y. Application of two dimensional orthogonal plate function to flexural vibrations of skew plates, *Journal of Sound and Vibration*, **139** (2), 241–252, (1990). https://dx.doi.org/10.1016/0022-460X(90)90885-4

9 Liew K. M., Xiang Y., Kitipornchai, S., and Wang, C. M. Vibration of thick skew plates based on Mindlin shear deformation plate theory, *Journal of Sound and Vibration*, **168** (1), 39–69, (1993). https://dx.doi.org/10.1006/jsvi.1993.1361

10 Basu, P. K., Rossow, M. P., and Szabo, B. A. Theoretical Manual and Users Guide for COMET-X, Report FRA/ORD-77/60, Washington University, (1977).

11 McGee, O. G. and Leissa, A. W. Three-dimensional free vibrations of thick skewed cantilevered plates, *Journal of Sound and Vibration*, **144** (2), 305–322, (1991). https://dx.doi.org/10.1016/0022-460X(91)90751-5

12 McGee, O. G., Leissa, A. W., and Huang, S.Vibrations of cantilevered skewed plates with corner stress singularities, *International Journal for Numerical Methods in Engineering*, **35** (2), 409–424, (1992). https://dx.doi.org/10.1002/nme.1620350211

13 Huang, C. S., McGee, O. G., Leissa, A. W., and Kim, J.W. Accurate vibration analysis of simply supported rhombic plates by considering stress singularities, *Journal of Vibration and Acoustics*, **117** (3A), 245–251, (1995). https://dx.doi.org/10.1115/1.2874440

14 McGee, O. G., Kim, J. W., Kim, Y. S., and Leissa, A. W. Corner stress singularity effects on the vibration of rhombic

plates with combinations of clamped and simply supported edges, *Journal of Sound and Vibration*, **193** (3), 555–580, (1996). https://dx.doi.org/10.1006/jsvi.1996.0302

[15] McGee, O. G., Kim, J. W., and Leissa A. W. The influence of corner stress singularities on the vibration characteristics of rhombic plates with combinations of simply supported and free edges, *Int. J. Mech. Sc.*, **41** (1), 17–41, (1999). https://dx.doi.org/10.1016/S0020-7403(97)00120-3

[16] Woo, K. S., Hong, C. H., Basu, P. K., and Seo, C. G. Free vibration of skew plates by p-version of F. E.M., *Journal of Sound and Vibration*, **268** (4), 637–656, (2003). https://dx.doi.org/10.1016/S0022-460X(02)01536-5

[17] Zhou, L. and Zheng, W. X. Vibration of skew plates by the MLS-Ritz method, *Internal Journal of Mechanical Sciences*, **50** (7), 1133–1141, (2008). https://dx.doi.org/10.1016/j.ijmecsci.2008.05.002

[18] Mizusawa, T. and Kondo, Y. Application of the spline element method to analyze vibration of skew Mindlin plates with varying thickness in one direction, *Journal of Sound and Vibration*, **241** (3), 485–501, (2001). https://dx.doi.org/10.1006/jsvi.2000.3303

[19] Malekzadeh, P. and Karami, G. Polynomial and harmonic differential quadrature methods for free vibration of variable thickness thick skew plates, *Engineering Structures*, **27** (10), 1563–74, (2005). https://dx.doi.org/10.1016/j.engstruct.2005.03.017

[20] Zhou, D., Lo, S. H., Au F. T. K., Cheung Y. K., and Liu W. Q. 3-D vibration analysis of skew thick plates using plates using Chebyshev-Ritz method, *International Journal of Mechanical Sciences*, **48** (12), 1481–93, (2006). https://dx.doi.org/10.1016/j.ijmecsci.2006.06.015

[21] Lai, S. K., Zhou, L., Zhang, Y. Y., and Xiang, Y. Application of the DSC-Element method to flexural vibration of skew plates with continuous and discontinuous boundaries, *Thin-Walled Structures*, **49** (9), 1080–1090, (2011). https://dx.doi.org/10.1016/j.tws.2011.03.019

[22] Wang, X. and Wu, Z. Differential quadrature analysis of free vibration of rhombic plates with free edges, *Applied Mathematics and Computation*, **225**, 171–183, (2013). https://dx.doi.org/10.1016/j.amc.2013.09.018

[23] Wang, X., Wang, Y., and Yuan, Z. Accurate vibration analysis of skew plates by the new version of the differential quadrature method, *Applied Mathematical Modelling*, **38** (3), 926–937, (2014). https://dx.doi.org/10.1016/j.apm.2013.07.021

[24] Stahl, B. and Keer, L. M. Vibration and stability of cracked rectangular plates, *International Journal of Solids and Structure*, **8** (1), 69–91, (1972). https://dx.doi.org/10.1016/0020-7683(72)90052-2

[25] Huang, C. S. and Leissa, A. W. Vibration analysis of rectangular plates with side cracks via the Ritz method, *Journal of Sound and Vibration*, **323** (3–5), 974–988, (2009). https://dx.doi.org/10.1016/j.jsv.2009.01.018

[26] Huang, C. S., Leissa, A. W., and Chan, C. W. Vibrations of rectangular plates with internal cracks or slits, *Internal Journal of Mechanical Sciences*, **53** (6), 436–445, (2011). https://dx.doi.org/10.1016/j.ijmecsci.2011.03.006

[27] Bachene, M., Tiberkak, R., and Rechak, S. Vibration analysis of cracked plates using the extended finite element method, *Archive of Applied Mechanics*, **79** (3), 249–262, (2009). https://dx.doi.org/10.1007/s00419-008-0224-7

[28] Israr, A., Manoach, E., Trendafilova, I., Ostachowicz, M., Krawczuk, M., and Zak, A. Analytical modeling and vibration analysis of partially cracked rectangular plates with different boundary conditions and loading, *Journal of Applied Mechanics*, **76**, (2009). https://dx.doi.org/10.1115/1.2998755

[29] Ismail, R. and Cartmell, M. P. An investigation into the vibration analysis of a plate with a surface crack of variable angular orientation, *Journal of Sound and Vibration*, **331** (12), 2929–2948, (2012). https://dx.doi.org/10.1016/j.jsv.2012.02.011

[30] Joshi, P. V., Jain, N. K., and Ramtekkar, G. D. Analytical modeling and vibration analysis of internally cracked rectangular plates, *Journal of Sound and Vibration*, **333** (22), 5851–5856, (2014). https://dx.doi.org/10.1016/j.jsv.2014.06.028

[31] Liew, K. M., Hung, K. C., and Lim, M. K. A solution method for analysis of cracked plates under vibration, *Engineering Fracture Mechanics*, **48** (3), 393–404, (1994). https://dx.doi.org/10.1016/0013-7944(94)90130-9

[32] Moes, N., Dolbow. J., and Belytschko, T. A finite element method for crack growth without remeshing, *International Journal of Numerical Methods in Engineering*, **46** (1), 131–50, (1999). https://dx.doi.org/10.1002/(SICI)1097-0207(19990910)46:1%3C131::AID-NME726%3E3.3.CO;2-A

[33] Bardell, N. S. The free vibration of skew plates using the hierarchical finite element method, *Computers & Structures*, **45** (5–6), 841–74, (1992). https://dx.doi.org/10.1016/0045-7949(92)90044-Z

[34] Singh, B. and Chakraverty, S. Flexural vibration of skew plates using boundary characteristic orthogonal polynomials in two variables, *Journal of Sound and Vibration*, **173** (2), 157–178. (1994) https://dx.doi.org/10.1006/jsvi.1994.1224